Interface thermal resistance at low contact pressure - laboratory and neutron experiments*,**

Matthias Bartosik[1],
Supervised by Prof. I.C. Noyan[2] and Dr. S.Y. Lee[2],
Advisor in Austria: Assoc. Prof. Jozef Keckes[1]

[1]Department of Materials Physics, Montanuniversität Leoben and Erich Schmid Institute for Materials Science, Austrian Academy of Sciences, Austria
[2]Columbia University, Applied Physics and Applied Mathematics, NY 10027

Abstract

A neutron experiment was performed at the VULCAN beamline [i] of the Oak Ridge National Laboratory to determine the thermal resistance of buried interfaces. In the experiment an aluminum block was placed between two temperature controlled aluminum plates (one heated, one cooled). By collecting diffraction patterns at different positions in the aluminum sandwich a temperature map was created, whereby the thermal expansion of the lattice parameter served as a temperature gauge. From the temperature distribution the thermal resistance of the aluminum interfaces can be evaluated. Complementary laboratory experiments were conducted to determine the influence of temperature, contact pressure and thermal paste on the thermal resistance of the buried interfaces. It was found that the total thermal resistance of the three aluminum plates decreases from 2.25×10^{-3} to 1.32×10^{-3}, 6.89×10^{-4} and 4.49×10^{-4} m²K/W when applying a contact pressure of 0.05MPa, thermal paste and both combined, respectively. Finite Element Method (FEM) simulations were carried out to confirm the experimental results. Finally, the constriction resistance R_s [ii] (at one interface) was estimated to be 1.33×10^{-3} m²K/W for the setup with a contact pressure of 0.05MPa.

Introduction

Neutron diffraction is an important tool for materials engineering and materials science. Due to the high penetration depth of neutron radiation full-size components (e.g. circumferential welds in 500 mm long segments of a 912 mm diameter pipe-line) can be characterized [iii].

Typical research areas that arouse the interest of neutron beamline users are (*cf.* [iii]): (I) *Strain mapping*, which is conducted to elucidate the stress distribution in parts such as welds. The stress information can be used to optimize the design of the investigated component. (II) *Intergranular strain* evaluation is used to determine for example intrinsic thermal strains or load-sharing capabilities in composite materials. (III) *Crystallographic texture* describes the distribution of crystallographic grain orientations and affects for instance the deformation behavior of metals. (IV) Neutrons are also used to study stress distribution in components as a result of *surface modifications* such as shot-peening. (V) In-situ studies on the *response of a loaded component* or *at an elevated temperature* or solid-state reactions within *chemical reaction vessels* can be performed using dedicated equipment and beamlines.

The Vulcan beamline at the Oak Ridge National Laboratory provides a load-frame capable of multi-axial loading and fatigue tests, a high-temperature vacuum furnace, a portable friction stir-welding machine and standard equipment. Figure 1 shows a computer model of the beamline with the key components.
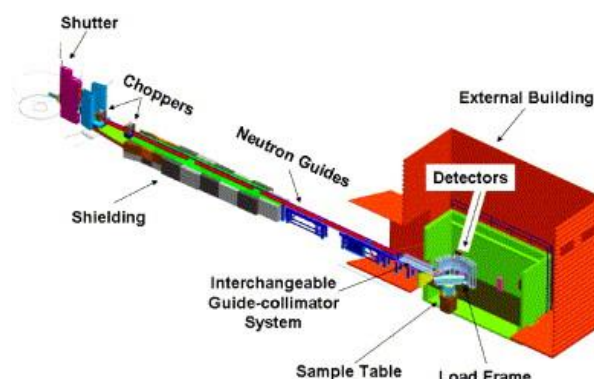

Fig. 1: 3D computer model of the VULCAN beamline [i]. The key components of the instrument are labeled.

Results from previous experiments

In 2010, Prof. Noyan's group conducted a neutron experiment at the Vulcan beamline of the Oak Ridge National Laboratory to measure the thermal resistance R of buried interfaces. The thermal resistance is important for heat transfer problems in various engineering applications and is defined as the temperature difference between the two solids in contact divided by the heat flux q:

$$R = \frac{\Delta T}{q} \qquad\qquad (1)$$

In the experiment three aluminum plates (one heated, one cooled and a middle plate) were brought into contact and kept together by springs (Fig. 2). Diffraction patterns were collected across the three plates (I) at room temperature and (II) during applying a temperature difference of 215°C between the hot and the cold plate. The hot plate was heated by cartridge heaters and the cold plate was cooled by liquid nitrogen. From the diffraction patterns the lattice parameter and thermal strain values ε_{th} were evaluated for different positions and converted into a temperature profile using the thermal expansion coefficient of aluminum α_{Al} (equation 2). The result of the experiment is depicted in Fig. 3.

$$\varepsilon_{th} = \frac{a - a_{RT}}{a_{RT}} = \alpha_{Al}(T - RT) \qquad\qquad (2)$$

FEM simulations were carried out to simulate the temperature profiles and to evaluate the interface thermal resistance. Further details about the initial experiment can be found in [iv].
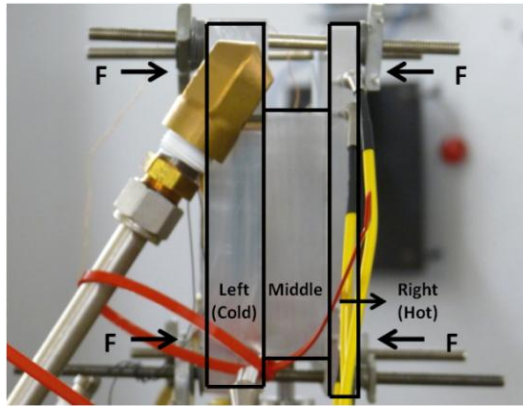
Fig. 2: Experimental setup of the neutron experiment [iv]. An aluminum plate is placed between a hot and a cold plate.
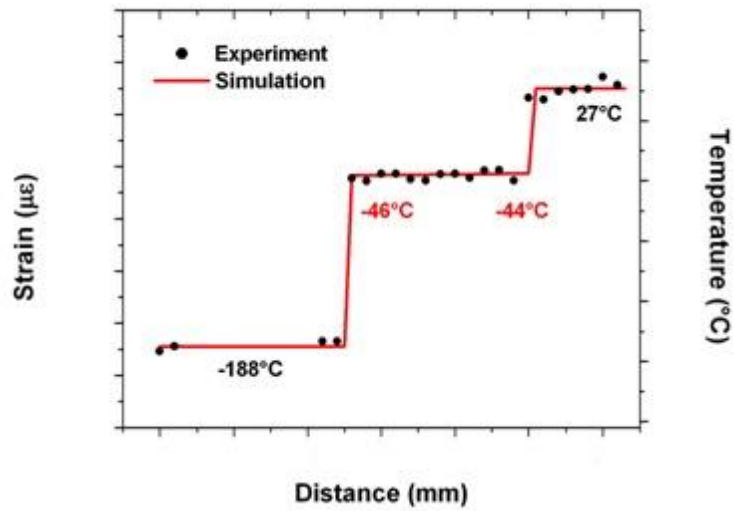

Fig. 3: From the expansion of the lattice parameter values the thermal strain profile was evaluated and converted into a temperature profile. At the interfaces a temperature drop can be observed [iv].

Research activities related to the research stay at the Columbia University

A follow-up neutron experiment was prepared. The experimental setup was modified and complementary laboratory experiments were performed to study the influence of temperature, thermal paste and contact pressure on the interface thermal resistance. The results were analyzed using analytical methods and FEM. Finally, the prepared neutron experiment was performed at the Vulcan beamline. Some of the results from the neutron experiment are presented in this report.

Experimental setup modifications

In order to directly measure the temperature distribution across the aluminum plates thermocouples were implemented. Moreover an additional cold reservoir (Fig. 4) was designed, which ran with chilled water (instead of liquid nitrogen). The cold reservoir was made of aluminum and had a cylindrical cavity that acted as the water reservoir. Two drilled holes fitted valves for the water in and outlet. Around the cavity there was a groove for an O-ring. On the top of the thick plate a thin cover plate was attached with screws. The cover plate and the O-Ring prevented the cooling system from water leakage.
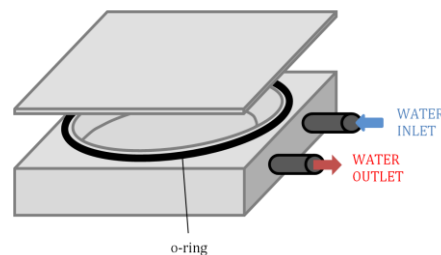

Fig. 4: Design of the cold reservoir made of aluminum, which ran with chilled water.

Systematic lab experiments

The influence of temperature, contact pressure and thermal paste on the interface thermal resistance was investigated. First the temperature of the cooling device was set to nominally 20°C and the temperature of the heating plate to 60, 80, 100, 120 and 140°C, respectively. At each temperature step the temperature was kept constant for about 30 min to ensure a steady state

condition. Besides the controller temperatures the temperature of the cooling and heating device near the interfaces and the temperature distribution in the middle plate were recorded for each temperature step. Subsequently the experiment was repeated but this time the contact pressure was modified by loading the setup with weights of a total mass of approximately 54 kg (530 N), which corresponded to a pressure of about 0.05MPa (area of the middle plate = 1.04×10^{-2} m^2).

In the next laboratory experiment thermal paste "OT-201 Thermally Conductive Silicone Paste" [v] was applied. Finally an additional load and thermal paste were applied simultaneously. The different experimental setups and the positions of the thermocouples are schematically presented in Fig. 5. In the setups with the additional weights a ceramic plate was inserted between the hot plate and the weights for insulation.
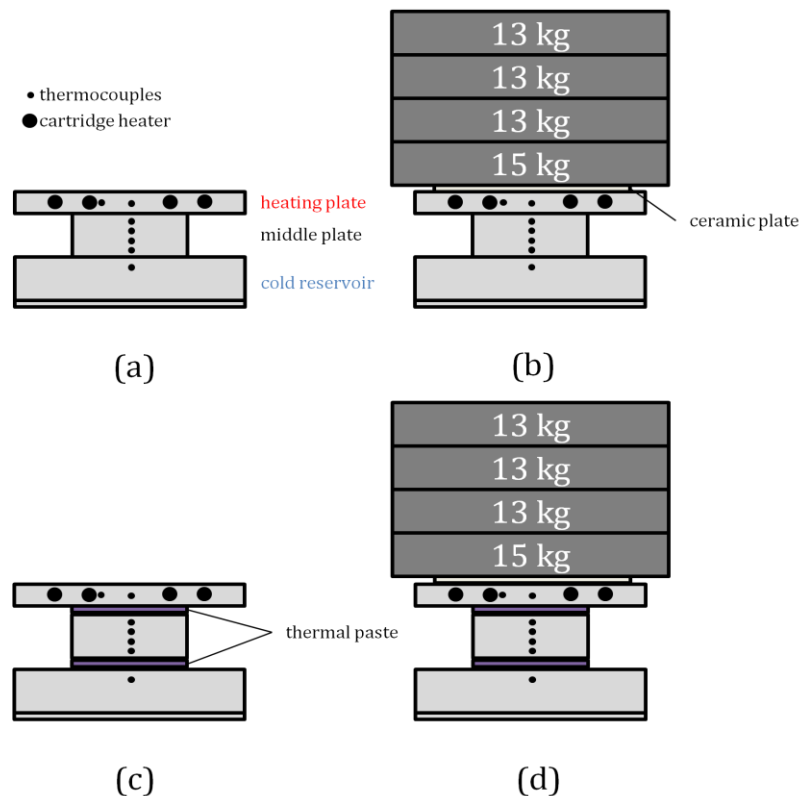

Fig. 5: (a) Experimental setup with the positions of the thermocouples and the cartridge heaters, (b) setup with additional weights to modify the contact pressure, (c) setup with thermal paste and (d) setup with additional weights and thermal paste (d).

Analytical Solution

Supposing that the thermal properties of the middle plate are constant and that there are no sources of thermal energy the steady state temperature distribution $T(x)$ in one dimension is a linear function satisfying the boundary conditions $T(x_1) = T_1$ and $T(x_2) = T_2$ [vi]. The temperature distribution is shown in Fig. 6a.
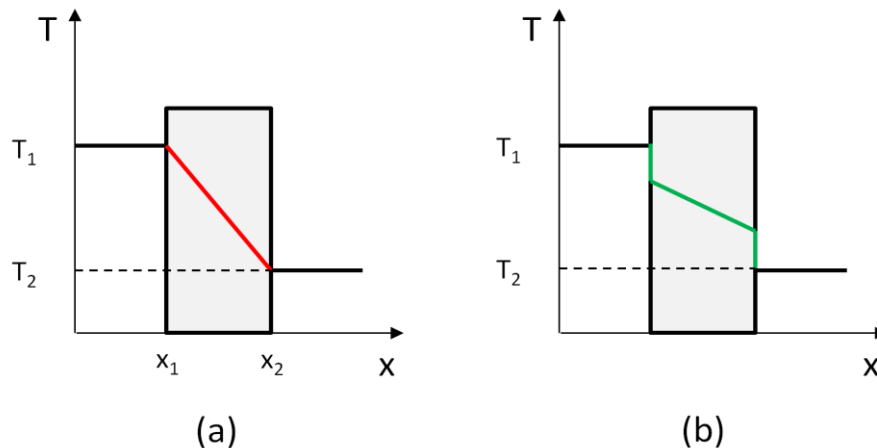

(a)   (b)

Fig. 6: Temperature distribution (a) without and (b) with interface thermal resistance.

In the case of heat conduction across interfaces a temperature drop can be observed (Fig. 6b). One way to account for the temperature drop is to model the interface as a thin virtual material which is inserted between the solids (Fig. 7). The virtual material exhibits the interface properties.
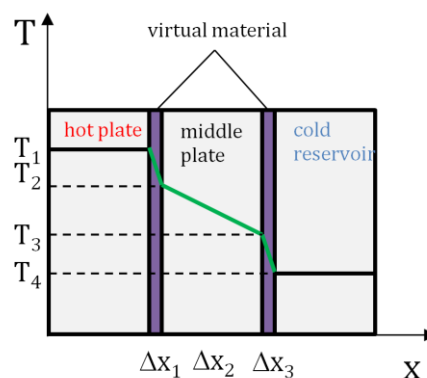

Fig. 7: Model of the three blocks in contact and the interfaces. A virtual material exhibiting the interface properties is inserted between the aluminum plates.

The heat flux through layers of different materials is described for instance in [vii]: Applying constant temperatures T_1 on the hot plate and T_4 on the cold plate $(T_1 > T_4)$ and assuming a steady state condition, results in a constant heat flux q through the virtual materials and the middle plate, that is $q_1 = q_2 = q_3 = q$. Inserting Fourier's law of heat conduction one can write the following equations, where k_1, k_2 and k_3 are the thermal conductivity values of the left interface, the middle plate and the right interface, respectively:

$$q = \frac{k_1}{\Delta x_1}(T_1 - T_2) \rightarrow q\left(\frac{\Delta x_1}{k_1}\right) = (T_1 - T_2) \qquad (3)$$

$$q = \frac{k_2}{\Delta x_2}(T_2 - T_3) \rightarrow q\left(\frac{\Delta x_2}{k_2}\right) = (T_2 - T_3) \qquad (4)$$

$$q = \frac{k_3}{\Delta x_3}(T_3 - T_4) \rightarrow q\left(\frac{\Delta x_3}{k_3}\right) = (T_3 - T_4) \qquad (5)$$

Summing up equations (3) – (5) leads to

$$q\left(\frac{\Delta x_1}{k_1} + \frac{\Delta x_2}{k_2} + \frac{\Delta x_3}{k_3}\right) = (T_1 - T_4) \qquad (6)$$

By inserting the definition of the thermal resistance $R = \frac{\Delta x}{k}$, equation (6) becomes:

$$q(R_1 + R_2 + R_3) = (T_1 - T_4) \qquad (7)$$

Equation (7) shows that the thermal resistance of the two interfaces and the middle plate add together similar to resistors in an electrical circuit which are connected in series. Assuming that both interfaces exhibit the same thermal properties, that is $R_1 = R_3 \equiv R_i$ and inserting $q=(T_2-T_3)/R_2$ leads to:

$$\frac{R_i}{R_2} = \frac{1}{2}\left(\frac{T_1-T_4}{T_2-T_3} - 1\right) \qquad (8)$$

The thermal resistance of the middle plate $R_2 = \frac{\Delta x_2}{k_2}$ is known so R_i can be calculated:

$$R_i = \frac{1}{2}\frac{\Delta x_2}{k_2}\left(\frac{T_1-T_4}{T_2-T_3}-1\right) \tag{9}$$

Thermal constriction resistance

In another approach by S.M.S. Wahid et al. [ii] the thermal constriction resistance across solid contact spots was used to describe the heat transfer across a joint. A real surface is never perfectly smooth, that is the interface of two nominally flat surfaces consists of actual contact spots separated by large gaps. The thermal constriction resistance can be estimated by:

$$R_s = h_s^{-1} = \left(\frac{k}{F}\left[\frac{1}{2\pi}\right]\left(\frac{\tan\theta}{R_q}\right)\exp\left[-\left\{\mathrm{erfc}^{-1}\left(\frac{2P}{H}\right)\right\}^2\right]\right)^{-1} \tag{10}$$

R_s solid spot resistivity of the actual contact spots ($m^2 K/W$)

h_s solid spot conductance through the actual contact spots ($W/m^2 K$)

k thermal conductivity of the solid

F constriction alleviation factor

$\tan\Theta$ mean absolute slope of the surface profile

R_q effective rms surface roughness

P applied pressure

H micro hardness (MPa)

Before applying (10) it should be confirmed that the plasticity index ψ_M [vii] is less than 0.33. The plasticity index ψ_M is defined as:

$$\psi_M = \frac{H}{(E' \tan\theta)} \tag{11}$$

where E' is the reduced elastic modulus for the materials in contact:

$$E' = 2\left[\left\{\frac{1-v_1^2}{E_1}\right\} + \left\{\frac{1-v_2^2}{E_2}\right\}\right]^{-1} \qquad\qquad (12)$$

Finite Element Method (FEM)

FEM simulations (ABAQUS-6.8) were carried out to simulate the temperature profiles across the aluminum sandwich. The model [iv] consisted of three solids exhibiting the thermal conductivity k = 167 W/mK of aluminum and two thin virtual solid materials which were inserted between the aluminum plates to model the interface properties. The interface thermal conductivity values were optimized so that the simulated temperature profile fitted best with the experimental data. The interface thickness was estimated as the sum of the RMS surface roughness values of the middle plate and the heating plate measured by an optical profilometer [iv]. An interface thickness of Δx = 2.4 µm was found. The finite element type was *linear heat transfer* (DC3D8). For the boundary temperatures the measured temperatures of the cooling device and the heating plate near the interfaces were applied on the left and the right aluminum plate, respectively.

Results and Discussion

The experimental data for the different setups and ΔT are depicted in Fig. 8. The temperatures in the middle plate followed a linear trend. The slope of the linear function was increasing along with the applied ΔT between hot and cold plate. Similar to the initial neutron experiments [iv] a temperature drop was observed at the interfaces.
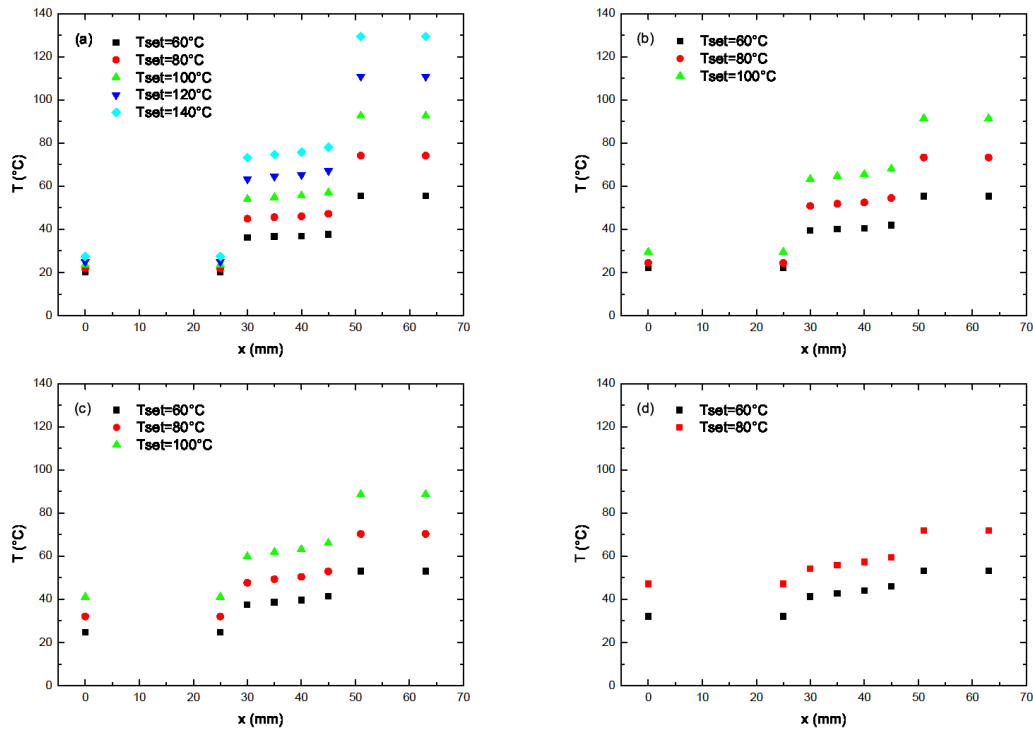
Fig. 8: (a) Temperature profiles of the setup loaded by the mass of the aluminum plates, (b) the setup with an additional contact pressure of 0.05MPa, (c) the setup with the thermal paste and (d) the setup with the additional pressure and the thermal paste combined. The temperature profiles were recorded for different ΔT values between the hot and the cold plate.

In Fig. 9 the temperature profiles of the four setups are compared for nominally the same boundary temperatures. The temperatures of the cold and the hot side near the interfaces deviated from the nominal temperatures. This effect became obviously more significant with increasing interface thermal conductivity. In addition the temperature profile became slightly asymmetric. In the FEM simulation the latter effect was taken into account by assigning different thermal conductivity values to the virtual materials.

The ratio of the interface thermal resistance to the thermal resistance of the bulk middle plate was evaluated using equation (8). For the temperatures T_2 and T_3 the linear extrapolated temperatures of the middle plate at the position of the interfaces were used. The results (Fig. 10) document that the ratio decreased from about 7 to 4 when applying an additional contact pressure of 0.05MPa, to 2

when using thermal paste and to about 1 when applying an additional contact pressure (0.05MPa) and thermal paste simultaneously.

Since the thermal resistance of the bulk middle plate was known the interface thermal resistance could be calculated using equation (9). A summary of the results is given in Table 1. The total thermal resistance was the sum of the two interface thermal resistance values and the bulk thermal resistance. The bulk thermal resistance $R_2 = \frac{\Delta x_2}{k_2}$ was about 1.5 x 10^{-4} m^{2}K/W when using a thickness of the middle plate of Δx_2 = 25 mm and a thermal conductivity k_2 = 167 W/mK. The total thermal resistance values for the different setups were approximately: 2.25 x 10^{-3}, 1.32 x 10^{-3}, 6.89 x 10^{-4} and 4.49 x 10^{-4} m^{2}K/W. Thus the additional contact pressure reduced the total thermal resistance to about 60%, the thermal paste to about 30% and both combined to about 20% of the total thermal resistance of the setup with the bare aluminum plates.
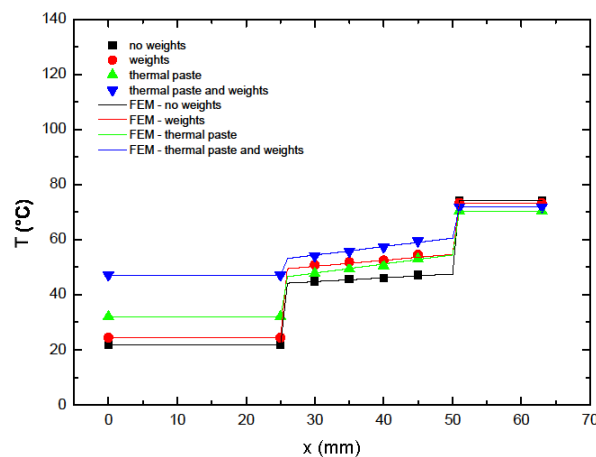

Fig. 9: Comparison of the temperature profiles and the FEM results for the four setups with nominally the same temperature difference between the hot and the cold side.
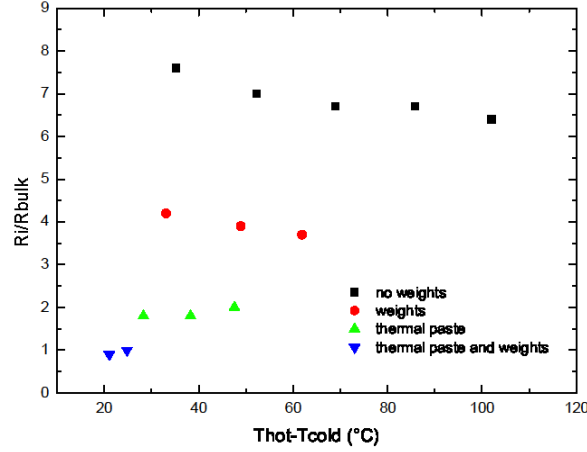
Fig. 10: Ratio of the interface thermal resistance to the bulk thermal resistance as a function of ΔT.

	condition	interface1	bulk	interface2	total
Analytical solution	bare Al plates	1.05×10^{-3}	1.50×10^{-4}	1.05×10^{-3}	2.25×10^{-3}
	pressure applied	5.84×10^{-4}	1.50×10^{-4}	5.84×10^{-4}	1.32×10^{-3}
	thermal paste	2.69×10^{-4}	1.50×10^{-4}	2.69×10^{-4}	6.89×10^{-4}
	pressure applied and thermal paste	1.50×10^{-4}	1.50×10^{-4}	1.50×10^{-4}	4.49×10^{-4}

Table 1: Comparision of the thermal resistance values obtained from the analytical solution in (m^2K/W).

For the setup with the applied load of 0.05MPa the thermal restriction resistance (at one interface) was found to be R_s **= 1.33 x 10^{-3} m^{2}K/W** when using equation (10). It was confirmed that the plasticity index ψ_M is under 0.33. In our case ψ_M was about 0.14. The following parameters were used: $E_1 = E_2$ = 68900MPa, $v_1 = v_2$ = 0.33, k = 167 W/mK, F = 1, $\tan\Theta \cong 0.13$, $R_q \cong 1.78$ μm, P = 0.05MPa, H = 1400MPa. Possible reasons for the difference between the analytical solution/FEM result ($R_{interface1} = R_{interface2}$ = 5.84 x 10^{-4}) and the thermal restriction resistance (R_s = 1.33 x 10^{-3}) are (I) the presence of natural aluminum oxide on the surface of the aluminum plates, (II) the scattering of the phonons and electrons, which carry the heat, on the grain boundaries of the polycrystalline material and (III) the relatively low applied contact pressure.

The neutron experiment was performed at the Vulcan beamline of the Spallation Neutron Source of the Oak Ridge National Laboratory. The three aluminum plates (hot, cold and middle plate) were kept together by springs and mounted vertically on the sample stages. The setup was rotated 45 deg from the incident beam and the detectors were positioned such that the lattice parameters of the aluminum plates were measured along Q_{IIx} and Q_{IIy} (Figs. 11 – 13).

Depth Scan

First, the setup with the bare three aluminum plates was measured at room temperature. By moving the sample stage along the _y_ direction (Fig. 13), neutron diffraction patterns at different positions were collected. This measurement served as a reference. In a next step a temperature difference between the hot and the cold plate was applied and the sample was scanned again. From each collected diffraction pattern the lattice parameter was evaluated using GSAS full pattern fitting. The thermal strain ε_{th} was then converted into temperature using the linear thermal expansion coefficient of aluminum α_{Al} (equation 2). During the neutron experiment the temperature distribution was also measured directly using the implemented thermocouples for a comparison. From the temperature distribution the interface thermal resistance can be determined (sec. _Analytical solution_, sec. _FEM_).

3D Temperature distribution

In this beamtime besides the "depth scans" a 3D map of the temperature distribution in the aluminum plates was created by collecting diffraction patterns from different positions (Fig. 14, 15). The data can be used to check the uniformity of the temperature distribution or to optimize heating or cooling devices.

Fig. 11: VULCAN beamline of the Oak Ridge National Laboratory. The setup was rotated 45 deg away from the incoming beam.
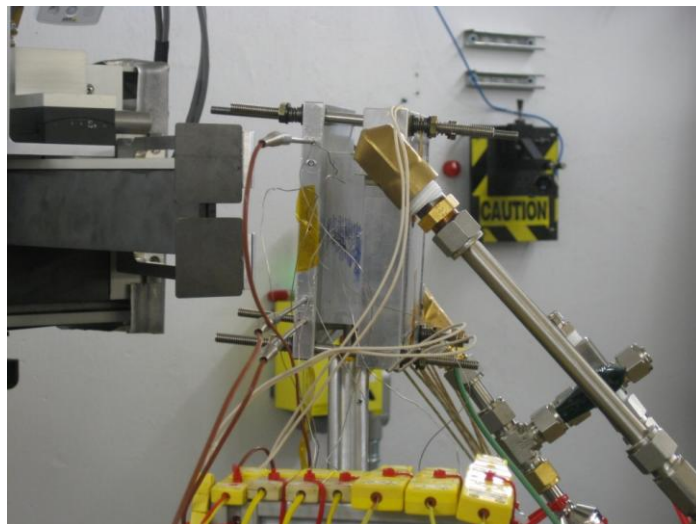

Fig. 12: Experimental setup. Hot side heated by cartridge heaters (left aluminum plate), middle plate and a cold reservoir cooled with liquid nitrogen (right aluminum plate). In contrast to the first neutron experiment multiple thermocouples were implemented in the setup to directly measure the temperature distribution.
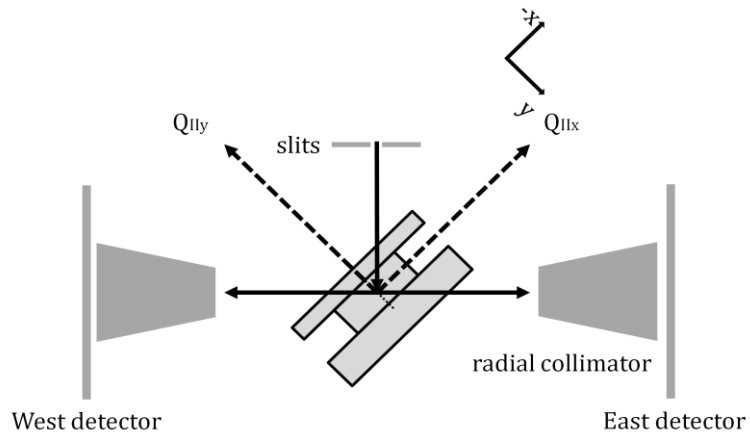
Fig. 13: Schematic diagram of the setup arrangement, redrawn and modified from [iv].
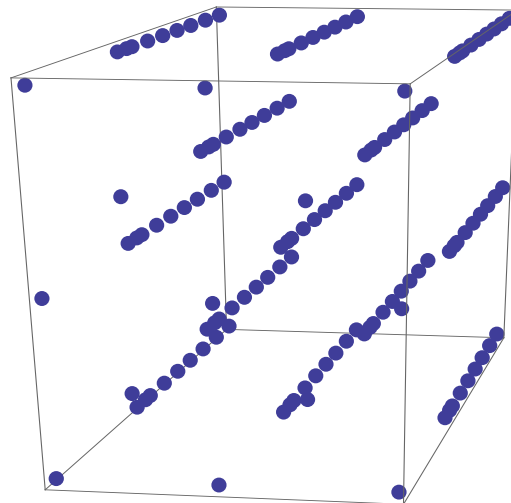

Fig. 14: At different positions (*x*, *y*, *z*) in all three plates (hot plate, cold plate and middle plates) diffraction pattern were collected. From the data the three dimensional temperature distribution can be evaluated.
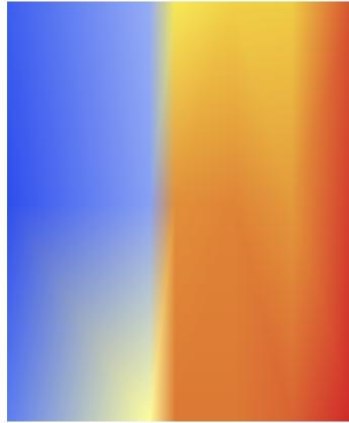
Fig. 15: Example of a temperature map through the aluminum sandwich – cooling plate (left), middle plate, hot plate (right).

Conclusions

The results from the neutron experiment demonstrate that a diffraction based method can be used to determine the temperature distribution inside full size components. The method is contactless and non-destructive. From the temperature distribution heat transfer problems related to various engineering applications can be investigated, e.g. the thermal resistance of buried interfaces. Complementary laboratory experiments using multiple thermocouples have shown that the total thermal resistance of the three aluminum plates in contact can be decreased to about 60, 30 and 20% when increasing the contact pressure (0.05MPa), when applying thermal paste and both combined, respectively.

Acknowledgements

Appendix

I. Statement of Research, Vulcan Proposal 2011 submitted by Prof. Noyan and Dr. Lee.

Measurement of Interface Thermal Resistance with Neutron Diffraction

I. Scientific Background

Interface thermal resistance is an important factor for engineering applications involving heat transfer. Measurement of this parameter across buried interfaces is problematic: heat flux measurement requires complicated apparatus, and depends on exact specification of multiple, hard-to-measure, variables including surface roughness, contact pressure, geometric configuration, directionality of heat flow etc.

We propose to test a new neutron-diffraction technique for measuring thermal resistance across buried interfaces using the Vulcan Instrument of the Spallation Neutron Source. This technique can be applied to all systems where diffraction can be used to measure lattice parameters. After validation in the initial set of experiments, we plan to use this technique for measuring the thermal conduction across heat sink interfaces in micro-electronic devices.
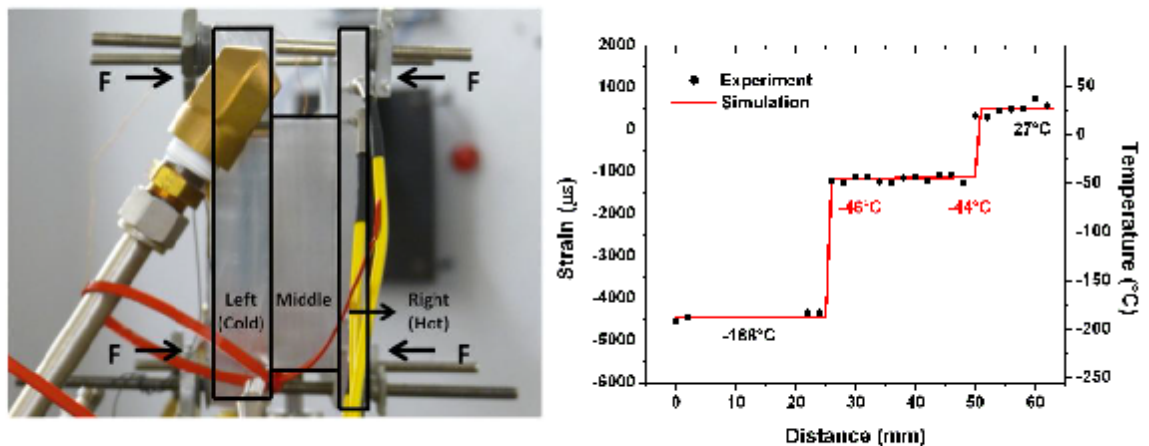
II. Results of Preliminary Work

Fig. 1. (a) Experimental setup of the Al block at VULCAN[1]. The left reservoir is cooled by liquid nitrogen. The right reservoir is heated by resistance type cartridge heaters. (b) strain profile from neutron diffraction experiment vs. finite element simulation with $\Delta T=215°C$. The temperature values on the right ordinate are from the finite element simulation, but can also be calculated directly from the thermal expansion coefficient function of Al[2].

We have conducted an initial experiment at VULCAN in November, 2010, where the lattice-parameter profile within an Al6061 block sandwiched between two temperature-controlled heat reservoirs (one cold, one hot) was measured as a function of position (Fig. 1). Two scans ($\Delta T=0$ and $\Delta T=215°C$) were performed. Rietveld full pattern refinement yielded position dependent precise lattice parameters. These were used to compute the thermal strain profile with position. The thermal strain across the Al-block was constant with position, and indicated constant temperature profile. Finite element simulation (ABAQUS-6.8) was carried out to link the observed strain profile to the boundary temperatures by optimizing thermal conductivity (k) values of the two interfaces. We observed that, in order to match the observed thermal strain profile, the interface thermal resistances approximately 10^{-6} of the bulk values were necessary (a journal article has been prepared and will be submitted to Journal of Applied Physics [1] by the end of March 2011).

III. Experiment Plan

We plan to measure position dependent lattice parameter studies across the Al block while changing the following parameters: 1) surface roughness (at constant pressure), 2) pressure (at constant surface roughness), 3) thermal transfer materials (at constant surface roughness and pressure).; for this purpose commercial thermal transfer materials such as silver paste and indium foil will be used. For further validation of the diffraction temperature measurements, thermocouples will be integrated into the middle plate in addition to the thermocouples in the heat sinks (this was not done in our initial experiments).

The smallest radial collimators available at VULCAN will be utilized for both detector banks and we will measure the Al lattice parameter through the plated depth at 1mm intervals. Each depth scan will require 6 hours. Including 1 day of setup and calibration, a total of 5 days of beam time is necessary to complete this experiment.

IV. Goal of Experiment

The basic experimental goal is to validate a diffraction-based technique of measuring the thermal resistance of buried interfaces. In addition, we plan to extend this technique to the measurement of absolute and spatial strain resolution of spallation neutron instruments[2].

[1]   Lee, S.Y., Noyan, I.C., Wang, X-L., An, K., Stoica, D. et. al " *Measurement of Interface Thermal Resistance with Neutron Diffraction*". To be submitted to Journal of Applied Physics, 2011.

[2]   Polvino, S.M, "*Accuracy Precision and Resolution in Strain Measurements on Diffraction Instruments*" PhD Thesis, Dept. of *Applied Physics and Applied Mathematics*. Columbia University: New York (2011).

[i] X.-L. Wang, T.M. Holden, G.Q. Rennich, A.D. Stoica, P.K. Liaw, H. Choo and C.R. Hubbard, "VULCAN--The engineering diffractometer at the SNS", *Physica B: Condensed Matter*, Volumes 385-386, Part 1, 2006.

[ii] S.M.S. Wahid, C.V. Madhusudana, E. Leonardi, "Solid spot conductance at low contact pressure", *Experimental Thermal and Fluid Science*, Volume 28, Issue 6, 2004.

[iii] T.M. Holden, SNS Report no. IS-1.7.9-6055-RE-A-00, http://neutrons.ornl.gov/instruments/SNS/VULCAN/pdf/science_case_for_vulcan.pdf

[iv] S.Y. Lee, I.C. Noyan, X.-L.Wang, et al. "Measurement of Interface Thermal Resistance with Neutron Diffraction". To be submitted to *Journal of Applied Physics*, 2011.

[v] http://www.omega.com/

[vi] Haberman, *"Applied Partial Differential Equations"*, Pearson Education, 4th Edition, 2003.

[vii] R. Raupenstrauch, "*Vorlesung zu Wärmetechnik*", Montanuniversität Leoben, 2002.

[viii] B.B. Mikic, "Thermal contact conductance, theoretical considerations", *International Journal of Heat and Mass Transfer* 17 (1974), 205-214.